

Σ and Ξ electromagnetic form factors in the extended vector meson dominance model


Bing Yan,^{1,2,*} Cheng Chen^{2,3,†} and Ju-Jun Xie^{2,3,4,‡}

¹College of Mathematics and Physics, Chengdu University of Technology, Chengdu 610059, China

²Institute of Modern Physics, Chinese Academy of Sciences, Lanzhou 730000, China

³School of Nuclear Sciences and Technology, University of Chinese Academy of Sciences, Beijing 101408, China

⁴Southern Center for Nuclear-Science Theory (SCNT), Institute of Modern Physics, Chinese Academy of Sciences, Huizhou 516000, Guangdong Province, China

 (Received 8 January 2023; revised 15 March 2023; accepted 23 March 2023; published 11 April 2023)

We propose a phenomenological extended vector meson dominance model for the baryon electromagnetic structure, and it is found that the current experimental data on the Σ and Ξ electromagnetic form factors in the timelike region can be well described. Meanwhile, we can also reproduce the ratios of the total cross sections of reactions $e^+e^- \rightarrow \Sigma^+\bar{\Sigma}^-$, $\Sigma^0\bar{\Sigma}^0$, and $\Sigma^-\bar{\Sigma}^+$, which are $9.7 \pm 1.3 : 3.3 \pm 0.7 : 1$ at center-of-mass energies from 2.3864 GeV to 3.02 GeV. We also analytically continue the expression of the form factors to spacelike region and estimate the charge radii of the Σ and Ξ hyperons. The obtained result of the charge radius for the Σ^- is in agreement with the experimental data.

DOI: [10.1103/PhysRevD.107.076008](https://doi.org/10.1103/PhysRevD.107.076008)

I. INTRODUCTION

The electromagnetic structure information of hadrons is characterized by the electromagnetic form factors (EMFFs), which are functions of the four-momentum transfer squared q^2 , with q the four-momentum carried by the exchanged virtual photon. Study of these EMFFs can lead to a better understanding of fundamental structure of hadrons. On the experimental side, most commonly the baryon EMFFs in the spacelike region ($q^2 < 0$) were measured in the electron-baryon scattering [1–4], while for these unstable hadrons, for example, these hyperons, their EMFFs in the spacelike region are very difficult to be experimentally measured. However, in the timelike region ($q^2 > 0$), their EMFFs can be measured through the electron-positron annihilation reactions by the BESIII and Belle Collaborations [5–12]. Meanwhile, the effective form factor $G_{\text{eff}}(q^2)$ of hyperons can be extracted from the high-precision measured Born cross sections of the reactions $e^+e^- \rightarrow Y\bar{Y}$ (Y stands for hyperon; \bar{Y} is anti-hyperon). It was pointed out that these baryon EMFFs in

the timelike region can be associated with the time evolution of the charge and magnetic distributions inside the baryon [13,14].

The hyperon effective form factors $G_{\text{eff}}(q^2)$ are the functions that parametrize the $\gamma Y\bar{Y}$ vertex generated by the strong interaction. Yet, the production vertex $\gamma Y\bar{Y}$ is very poorly understood so far [15,16]. The vector meson dominance (VMD) model is a very successful tool for studying the nucleon electromagnetic form factors, in both the spacelike and timelike regions [17–19]. Within a modified VMD model, the EMFFs of the Λ hyperon were investigated in Refs. [20,21]. By considering the $Y\bar{Y}$ final state interactions, the EMFFs of hyperons in the timelike region have been studied in Ref. [22]. It is worth to mention that the enhancement of the effective form factor of the Λ hyperon seen in the $e^+e^- \rightarrow \Lambda\bar{\Lambda}$ reaction was reproduced within the two above different calculations in Refs. [20,21] and Ref. [22], respectively. In the vector meson dominance model for studying the electromagnetic form factors of baryons, there is a phenomenological intrinsic form factor $g(q^2)$. From these studies of the nucleon and hyperon EMFFs [17–29], it is found that a better choice of $g(q^2)$ is the dipole form

$$g(q^2) = \frac{1}{(1 - \gamma q^2)^2}, \quad (1)$$

with γ a free parameter. In the spacelike region, the dipole form is consistent with the results obtained from perturbative quantum chromodynamics calculations [30,31]. In the

*yanbing@impcas.ac.cn

†chencheng22@mails.ucas.ac.cn

‡xiejujun@impcas.ac.cn

Published by the American Physical Society under the terms of the [Creative Commons Attribution 4.0 International license](https://creativecommons.org/licenses/by/4.0/). Further distribution of this work must maintain attribution to the author(s) and the published article's title, journal citation, and DOI. Funded by SCOAP³.

TABLE I. Values of γ (in GeV^{-2}) for octet baryons used in previous works.

	Proton ([17–19])	Neutron ([24–27])	Λ ([20])	Λ ([21])
γ	1.408	1.408	0.336	0.48 ± 0.08
	Σ^+ ([32])	Σ^- ([32])	Σ^0 ([27])	Ξ^0 ([27])
γ	0.46 ± 0.01	1.18 ± 0.13	0.26 ± 0.01	0.21 ± 0.02

timelike region, it should be noticed that γ is a positive parameter, thus $g(q^2)$ will have a pole in the position $\gamma = 1/q^2$. Such pole could be restricted in the unphysical region, if γ satisfies $\gamma > 1/(4m_Y^2)$ for hyperon Y .

For a long time, the simple dipole form parametrization was very useful for the discussion of different baryons. For example, the dipole form of $g(q^2)$ can well describe the effective form factors of Λ [20,21], Σ [32], and Ξ [27], while for the nucleon, a good general review is given in Refs. [33–36], both from the theoretical and from the experimental points of view. However, these determined values of γ for different ground state octet baryons with spin 1/2 are very different, even for the triplet Σ^+ , Σ^- and Σ^0 [32]. The determined values of γ , from previous works, for nucleon, Λ , Σ , and Ξ^0 baryons are collected in Table I. Nevertheless, the VMD model and the parametrization of $g(q^2)$ can give a reasonable description of the experimental data on the baryon EMFFs at the considered energy region.

Various experimental and theoretical efforts have been contributed to the electromagnetic form factors. Very recently, the EMFFs of Σ^+ , Σ^- , and Σ^0 hyperons in the timelike region have been measured with high precision by the BESIII Collaboration through $e^+e^- \rightarrow \Sigma^+\bar{\Sigma}^-$ [9], $\Sigma^-\bar{\Sigma}^+$ [9], and $\Sigma^0\bar{\Sigma}^0$ reactions [10] at center-of-mass energies from 2.3864 GeV to 3.02 GeV. The resulting ratios of total cross sections of these above three reactions are $9.7 \pm 1.3:1:3.3 \pm 0.7$ [9,37,38], which disagree with various theoretical model predictions [39,40]. After the experimental measurements of $e^+e^- \rightarrow \Sigma^+\bar{\Sigma}^-$ and $\Sigma^-\bar{\Sigma}^+$ [9], the effective form factors of Σ^+ and Σ^- were investigated by using the VMD model [32], where the parameter γ was taken with different values for Σ^+ and Σ^- . In Ref. [22], by considering the final state interactions of $Y\bar{Y}$, the energy dependence of the three reactions $e^+e^- \rightarrow \Sigma^+\bar{\Sigma}^-$, $\Sigma^0\bar{\Sigma}^0$, and $\Sigma^-\bar{\Sigma}^+$ at low energies can be roughly reproduced, and it was found that there is a strong interplay between $\Sigma^+\bar{\Sigma}^-$, $\Sigma^0\bar{\Sigma}^0$, and $\Sigma^-\bar{\Sigma}^+$ channel in the near-threshold region, caused by the $\Sigma\bar{\Sigma}$ final-state interactions.

In the present work, we revisit the EMFFs in the timelike region of Σ and Ξ hyperons within an extended vector meson dominance model, where the effects of the isospin combinations from isovector ρ^0 and isoscalar ω and ϕ mesons are taken into account. Furthermore, we assume that the values of model parameter γ are the same for Σ and Ξ hyperons. In addition, a vector meson with mass around

2.7 GeV was considered for the sake of better fitting the EMFFs of the Ξ^0 and Ξ^- hyperons. We then progress to an analysis of the electromagnetic form factors in the spacelike region and evaluate the electromagnetic radius of Σ hyperons. The theoretical result for the Σ^- hyperon is in agreement with the experimental measurements.

This article is organized as follows: in the next section we will show the theoretical formalism of the Σ and Ξ electromagnetic form factors in the VMD model. Numerical results about the effective form factors of Σ and Ξ and total cross sections of $e^+e^- \rightarrow \Sigma\bar{\Sigma}$ and $\Xi\bar{\Xi}$ are shown in Sec. III, and a short summary is given in the final section.

II. FORMALISM

As already pointed out, at fixed-energy e^+e^- colliders, the EMFFs of hyperons in the timelike region were extracted from the data on the differential cross section of the process $e^+e^- \rightarrow Y\bar{Y}$. For analysis of the data, the BESIII Collaboration used the energy scan method [41–43], while the initial state radiation method was used by Belle Collaboration [12] and BABAR collaboration [44,45]. Besides, the effective form factors G_{eff} can be easily obtained from the data of the total cross sections. The module squared of effective form factor $|G_{\text{eff}}|^2$ is a linear combination of $|G_E|^2$ and $|G_M|^2$, and proportional to the total cross section of $e^+e^- \rightarrow Y\bar{Y}$ reaction. In this work, we study the EMFFs of Σ and Ξ baryons in the timelike region with the experimental measurements on the $e^+e^- \rightarrow Y\bar{Y}$ reactions. Based on parity conservation and Lorentz invariance, the electromagnetic current of the baryons with a spin of 1/2 characterize two independent scalar functions $F_1(q^2)$ and $F_2(q^2)$ depending on q^2 , which are the Dirac and Pauli form factors, respectively. Then the corresponding electrical and magnetic form factors $G_E(q^2)$ and $G_M(q^2)$ are written as [38,46,47],

$$G_E(q^2) = F_1(q^2) + \tau F_2(q^2), \quad (2)$$

$$G_M(q^2) = F_1(q^2) + F_2(q^2), \quad (3)$$

where M is the baryon mass and $\tau = q^2/(4M^2)$. With $G_E(q^2)$ and $G_M(q^2)$, the magnitude of the effective form factor $|G_{\text{eff}}(q^2)|$ is defined as

$$|G_{\text{eff}}(q^2)| = \sqrt{\frac{2\tau|G_M(q^2)|^2 + |G_E(q^2)|^2}{1 + 2\tau}}. \quad (4)$$

In the timelike region, the effective form factors of hyperons are experimentally studied via the electron-positron annihilation processes. Under the one photon exchange approximation, the total cross section of the

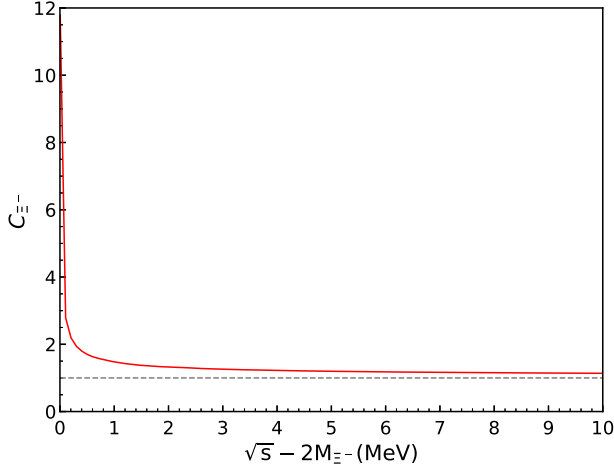


FIG. 1. The Coulomb factor for Ξ^- . The dashed horizontal line stands for $C_{\Xi^-} = 1$.

annihilation reaction $e^+e^- \rightarrow \bar{Y}Y$ can be expressed in terms of the effective form factor G_{eff} as [44,48,49]

$$\sigma_{e^+e^- \rightarrow \bar{Y}Y} = \frac{4\pi\alpha^2\beta C_Y}{3s} \left(1 + \frac{1}{2\tau}\right) |G_{\text{eff}}(s)|^2, \quad (5)$$

with $\alpha = e^2/(4\pi) = 1/137.036$ the fine-structure constant, and $\beta = \sqrt{1 - 4M_Y^2/s}$ is a phase-space factor. Here, $s = q^2$ is the invariant mass square of the e^+e^- system. The coulomb enhancement factor C_Y ¹ accounts for the electromagnetic interaction of charged pointlike fermion pairs in the final state [50], which is given by

$$C_Y = \begin{cases} \frac{y}{1-e^{-y}} & \text{for } \Sigma^+, \Sigma^-, \text{ and } \Xi^-, \\ 1 & \text{for } \Sigma^0 \text{ and } \Xi^0, \end{cases} \quad (6)$$

with $y = \frac{\alpha\pi}{\beta} \frac{2M_Y}{\sqrt{s}}$. Considering the C_Y factor, it is expected that the cross section of process $e^+e^- \rightarrow Y\bar{Y}$ is nonzero at the reaction threshold for charged hyperons pairs. As plotted in Fig. 1 for the case of Ξ^- ,² one can see that the factor C_Y affects only at the energy region very close to the reaction threshold. Moreover, it decreases very quickly as the reaction energy growing and it follows that few MeV above the reaction threshold it is $C_Y \sim 1$, then its effect can be safely neglected [50–53].

A. The EMFFs of Σ hyperon

In the VMD model, for the $e^+e^- \rightarrow \Sigma\bar{\Sigma}$ reaction, the virtual photon couples to Σ and $\bar{\Sigma}$ through isovector ρ^0 meson and isoscalar ω and ϕ mesons. Since both the ω and ϕ are far from the mass threshold of $\Sigma\bar{\Sigma}$, the behavior of the contributions from them are similar, thus we combine their

contributions. In this way, one can parametrize Dirac and Pauli form factors for Σ^+ and Σ^- in the timelike region as follows [17,19],³

$$F_1^{\Sigma^+} = g(q^2) \left(f_1^{\Sigma^+} + \frac{\beta_\rho}{\sqrt{2}} B_\rho - \frac{\beta_{\omega\phi}}{\sqrt{3}} B_{\omega\phi} \right), \quad (8)$$

$$F_2^{\Sigma^+} = g(q^2) \left(f_2^{\Sigma^+} B_\rho - \frac{\alpha_{\omega\phi}}{\sqrt{3}} B_{\omega\phi} \right), \quad (9)$$

$$F_1^{\Sigma^-} = g(q^2) \left(f_1^{\Sigma^-} - \frac{\beta_\rho}{\sqrt{2}} B_\rho - \frac{\beta_{\omega\phi}}{\sqrt{3}} B_{\omega\phi} \right), \quad (10)$$

$$F_2^{\Sigma^-} = g(q^2) \left(f_2^{\Sigma^-} B_\rho - \frac{\alpha_{\omega\phi}}{\sqrt{3}} B_{\omega\phi} \right), \quad (11)$$

$$F_1^{\Sigma^0} = g(q^2) \left(\frac{\beta_{\omega\phi}}{\sqrt{3}} - \frac{\beta_{\omega\phi}}{\sqrt{3}} B_{\omega\phi} \right), \quad (12)$$

$$F_2^{\Sigma^0} = g(q^2) \mu_{\Sigma^0} B_{\omega\phi}, \quad (13)$$

with

$$B_\rho = \frac{m_\rho^2}{m_\rho^2 - q^2 - im_\rho\Gamma_\rho}, \quad (14)$$

$$B_{\omega\phi} = \frac{m_{\omega\phi}^2}{m_{\omega\phi}^2 - q^2 - im_{\omega\phi}\Gamma_{\omega\phi}}, \quad (15)$$

where the widths of ρ , ω and ϕ are taken into account. In this work, we take $m_\rho = 0.775$ GeV, $\Gamma_\rho = 149.1$ MeV, $\Gamma_{\omega\phi} = (\Gamma_\omega + \Gamma_\phi)/2 = 6.4645$ MeV, and $m_{\omega\phi} = (m_\omega + m_\phi)/2 = 0.9005$ GeV, which are quoted in the review of particle physics book [54].

In addition, at $q^2 = 0$, with the constraints $G_E^{\Sigma^+} = 1$ and $G_M^{\Sigma^+} = \mu_{\Sigma^+}$, $G_E^{\Sigma^-} = -1$ and $G_M^{\Sigma^-} = \mu_{\Sigma^-}$, the coefficients $f_1^{\Sigma^+}$ and $f_2^{\Sigma^+}$, $f_1^{\Sigma^-}$, and $f_2^{\Sigma^-}$ can be calculated,

$$f_1^{\Sigma^+} = 1 - \frac{\beta_\rho}{\sqrt{2}} + \frac{\beta_{\omega\phi}}{\sqrt{3}}, \quad f_2^{\Sigma^+} = \mu_{\Sigma^+} - 1 + \frac{\alpha_{\omega\phi}}{\sqrt{3}}, \quad (16)$$

³We have followed:

$$\begin{aligned} |\Sigma^+\bar{\Sigma}^- \rangle &= \frac{1}{\sqrt{2}} |1, 0\rangle + \frac{1}{\sqrt{3}} |0, 0\rangle + \frac{1}{\sqrt{6}} |2, 0\rangle, \\ |\Sigma^-\bar{\Sigma}^+ \rangle &= -\frac{1}{\sqrt{2}} |1, 0\rangle + \frac{1}{\sqrt{3}} |0, 0\rangle + \frac{1}{\sqrt{6}} |2, 0\rangle, \\ |\Sigma^0\bar{\Sigma}^0 \rangle &= -\frac{1}{\sqrt{3}} |0, 0\rangle + \sqrt{\frac{2}{3}} |2, 0\rangle, \end{aligned} \quad (7)$$

with the basis of $|I_{\Sigma\Sigma}, I_{\Sigma\Sigma}^Z \rangle$. In the one photon exchange approximation, there is no contributions from the isospin tensor terms.

¹It is also called Sommerfeld factor.

²The numerical results for Σ^+ and Σ^- are similar.

$$f_1^{\Sigma^-} = -1 + \frac{\beta_\rho}{\sqrt{2}} + \frac{\beta_{\omega\phi}}{\sqrt{3}}, \quad f_2^{\Sigma^-} = \mu_{\Sigma^-} + 1 + \frac{\alpha_{\omega\phi}}{\sqrt{3}}. \quad (17)$$

In this work, we take $\mu_{\Sigma^+} = 3.112\hat{\mu}_{\Sigma^+}$, $\mu_{\Sigma^-} = -1.479\hat{\mu}_{\Sigma^-}$, $\mu_{\Sigma^0} = 2.044\hat{\mu}_{\Sigma^0}$ in natural unit [54], i.e., $\hat{\mu} = \frac{e}{2M_\Sigma}$.

Finally, the model parameters γ , the coefficients β_ρ , $\beta_{\omega\phi}$, and $\alpha_{\omega\phi}$ will be determined by fitting them to the experimental data on the timelike effective form factors of Σ^+ , Σ^0 , and Σ^- , which will be discussed in following.

B. The EMFFs of Ξ hyperon

For the case of $e^+e^- \rightarrow \Xi^-\Xi^+$ and $\Xi^0\Xi^0$ reactions, since Ξ^- and Ξ^0 are isospin doublets, we express the $\Xi^-\Xi^+$ and $\Xi^0\Xi^0$ states in terms of isospin 0 and 1 components. The mixtures of isoscalar and isovector for $\Xi^-\Xi^+$ and $\Xi^0\Xi^0$ of equal relative weight but different sign are imposed by the isospin symmetry as introduced by the underlying Clebsch-Gordan coefficients [54]. Then, the Dirac and Pauli form factors F_1 and F_2 for Ξ^- and Ξ^0 can be easily obtained as before for the Σ hyperon,

$$F_1^{\Xi^-} = g(q^2) \left(f_1^{\Xi^-} - \frac{\beta_\rho}{\sqrt{2}} B_\rho - \frac{\beta_{V_1}}{\sqrt{2}} B_{V_1} - \frac{\beta_{V_2}}{\sqrt{2}} B_{V_2} + \frac{\beta_{\omega\phi}}{\sqrt{2}} B_{\omega\phi} \right), \quad (18)$$

$$F_2^{\Xi^-} = g(q^2) \left(f_2^{\Xi^-} B_\rho - \frac{\alpha_{V_1}}{\sqrt{2}} B_{V_1} - \frac{\alpha_{V_2}}{\sqrt{2}} B_{V_2} + \frac{\alpha_{\omega\phi}}{\sqrt{2}} B_{\omega\phi} \right), \quad (19)$$

$$F_1^{\Xi^0} = g(q^2) \left(f_1^{\Xi^0} + \frac{\beta_\rho}{\sqrt{2}} B_\rho + \frac{\beta_{V_1}}{\sqrt{2}} B_{V_1} + \frac{\beta_{V_2}}{\sqrt{2}} B_{V_2} + \frac{\beta_{\omega\phi}}{\sqrt{2}} B_{\omega\phi} \right), \quad (20)$$

$$F_2^{\Xi^0} = g(q^2) \left(f_2^{\Xi^0} B_\rho + \frac{\alpha_{V_1}}{\sqrt{2}} B_{V_1} + \frac{\alpha_{V_2}}{\sqrt{2}} B_{V_2} + \frac{\alpha_{\omega\phi}}{\sqrt{2}} B_{\omega\phi} \right), \quad (21)$$

with

$$B_{V_1} = \frac{M_{V_1}^2}{M_{V_1}^2 - q^2 - iM_{V_1}\Gamma_{V_1}}, \quad (22)$$

$$B_{V_2} = \frac{M_{V_2}^2}{M_{V_2}^2 - q^2 - iM_{V_2}\Gamma_{V_2}}, \quad (23)$$

where we have considered contributions from two more excited vector mesons, V_1 and V_2 , in addition to the

contributions from ground states ρ , ω and ϕ . Their mass and width are M_{V_1} (M_{V_2}) and Γ_{V_1} (Γ_{V_2}), respectively. The mass M_{V_2} and width Γ_{V_2} are taken as used in Ref. [7], which are $M_{V_2} = 2.993$ GeV and $\Gamma_{V_2} = 88$ MeV. Besides, the coefficients $f_1^{\Xi^-}$, $f_2^{\Xi^-}$, $f_1^{\Xi^0}$, and $f_2^{\Xi^0}$ can be calculated as

$$f_1^{\Xi^-} = -1 + \frac{\beta_\rho}{\sqrt{2}} + \frac{\beta_{V_1}}{\sqrt{2}} + \frac{\beta_{V_2}}{\sqrt{2}} - \frac{\beta_{\omega\phi}}{\sqrt{2}}, \quad (24)$$

$$f_2^{\Xi^-} = \mu_{\Xi^-} + 1 + \frac{\alpha_{V_1}}{\sqrt{2}} + \frac{\alpha_{V_2}}{\sqrt{2}} - \frac{\alpha_{\omega\phi}}{\sqrt{2}}, \quad (25)$$

$$f_1^{\Xi^0} = -\frac{\beta_\rho}{\sqrt{2}} - \frac{\beta_{V_1}}{\sqrt{2}} - \frac{\beta_{V_2}}{\sqrt{2}} - \frac{\beta_{\omega\phi}}{\sqrt{2}}, \quad (26)$$

$$f_2^{\Xi^0} = \mu_{\Xi^0} - \frac{\alpha_{V_1}}{\sqrt{2}} - \frac{\alpha_{V_2}}{\sqrt{2}} - \frac{\alpha_{\omega\phi}}{\sqrt{2}}. \quad (27)$$

We take $\mu_{\Xi^-} = -0.915\hat{\mu}_{\Xi^-}$, and $\mu_{\Xi^0} = -1.749\hat{\mu}_{\Xi^0}$ in natural unit [54].

The parameter γ will be fixed as the one determined from the case of Σ , while the other free parameters $\beta_{\omega\phi}$, β_ρ , β_{V_1} , β_{V_2} , $\alpha_{\omega\phi}$, α_{V_1} , α_{V_2} , Γ_{V_1} , and M_{V_1} are determined by fitting them to experimental data on the timelike effective form factors of Ξ^- and Ξ^0 .

III. NUMERICAL RESULTS

Under the above formulations, we perform a four-parameter ($\gamma, \beta_\rho, \beta_{\omega\phi}, \alpha_{\omega\phi}$)- χ^2 fit to the experimental data on the effective form factors G_{eff} of Σ^+ , Σ^0 , and Σ^- hyperons. There are 33 data points in total, which are extracted at the center-of-mass energies from 2.3864 GeV to 3.0200 GeV. The fitted parameters are $\gamma = 0.527 \pm 0.024$ GeV⁻², $\beta_\rho = 1.63 \pm 0.07$, $\beta_{\omega\phi} = -0.08 \pm 0.06$, and $\alpha_{\omega\phi} = -3.18 \pm 0.77$. The fitted value of γ is consistent with the one obtained in Ref. [21] for the case of hyperon Λ . However, it is different with the value for Σ^- obtained in Ref. [32], where the effect of the isospin combination is not considered. The obtained χ^2/dof is 1.69, where dof is the number of dimension of the freedom. Note that the obtained χ^2/dof is larger than 1, since we have fitted all the experimental data from BESIII [9,10], Belle [12], and BABAR [45] Collaborations, by considering these contributions from only ground state of vector mesons. If we considered only these data of BESIII Collaboration [9,10], the obtained χ^2/dof is 1.17.

In Fig. 2 we show the theoretical results of the effective form factors of the Σ^+ , Σ^0 , and Σ^- . The red, blue, and green curves stand for the results for Σ^+ , Σ^0 , and Σ^- , respectively. The band accounts for the corresponding 68% confidence level (CL) interval deduced from the distributions of the fitted parameters. The experimental data from BESIII [9,10], Belle [12], and BABAR Collaboration [45] are also shown for comparing. One can see that, with same model parameters, we can describe these data on the effective

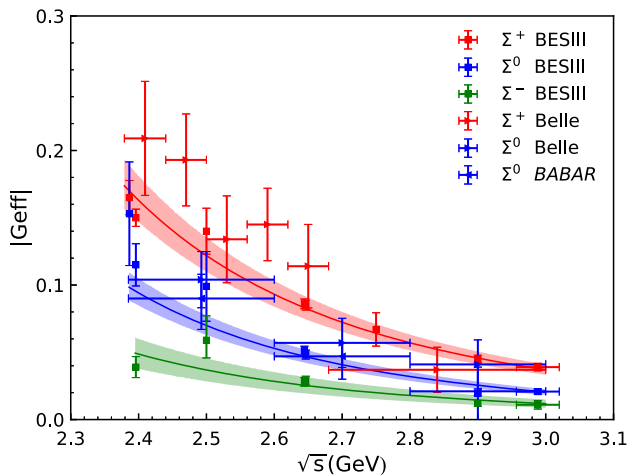


FIG. 2. The obtained effective form factors of Σ^+ , Σ^0 , and Σ^- , compared with the experimental data. The bands account for the corresponding 68% confidence-level interval deduced from the distributions of the fitted parameters.

form factors of Σ^+ , Σ^0 and Σ^- quite well, especially for the precise data measured by the BESIII Collaboration [9,10].

The total cross sections of $e^+e^- \rightarrow \Sigma\bar{\Sigma}$ are also calculated with these fitted parameters. The numerical results are shown in Fig. 3, compared with the experimental data. Since the effective form factors of Σ hyperons can be well reproduced with our model, the total cross sections of $e^+e^- \rightarrow \Sigma^+\bar{\Sigma}^-$, $e^+e^- \rightarrow \Sigma^0\bar{\Sigma}^0$ and $e^+e^- \rightarrow \Sigma^-\bar{\Sigma}^+$ reactions can be also well described. Again, the 68% CL bands are also shown.

For the case of Ξ^- and Ξ^0 effective form factors, γ is taken as the result of fitting to Σ hyperon, i.e., $\gamma = 0.527$. Then we have performed three different χ^2 fits (A, B, and C) to the

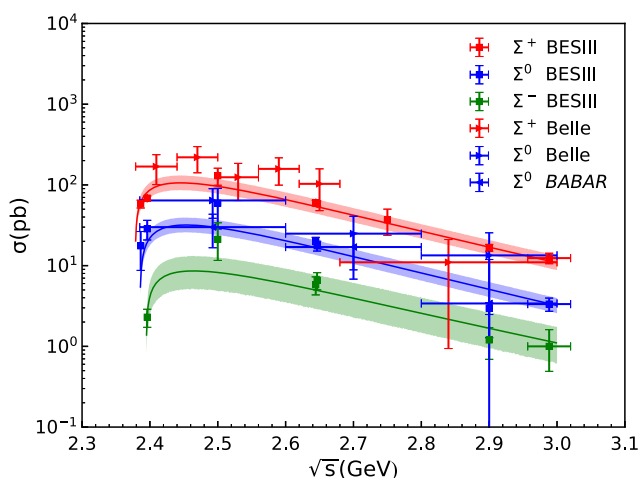


FIG. 3. The total cross section of Σ^+ , Σ^0 , and Σ^- hyperons compared with experimental data. The bands account for the corresponding 68% confidence-level interval deduced from the distributions of the fitted parameters.

experimental data on the effective form factors of the Ξ baryons. There are in total 18 data points, and these data correspond to the center-of-mass energies from 2.644 GeV to 3.080 GeV. For fit A, neither V_1 or V_2 is included. Only V_2 is considered in fit B. Both V_1 and V_2 are taken into account in fit C. The fitted parameters and corresponding χ^2/dof are compiled in Table II. One can see that, the χ^2/dof of fit C is much smaller than the other two fits, and it is rather small. This is because that there are too few data points around the V_1 peak. With the increase of parameters in fit C, the χ^2/dof becomes very low. Yet, with more data points being taken by the experiments around the relevant mass region, motivated by the theoretical studies here, the χ^2/dof for fit C is expected to become more natural, around one.

For the case of fit B, where V_1 is not included, it is found that the corresponding fitted results of effective form factors of Ξ^0 cannot be well reproduced, especially for the two data points around 2.7 GeV and 2.8 GeV. Thus, a new vector state around 2.742 GeV should be needed.

For fit C, there are nine free parameters. Since we have more free parameters and the experimental data points are limited, the uncertainties of these parameters obtained from the χ^2 fit are much large. To get reasonable errors for these model parameters, for instance, the parameter β_{V_1} , we do the following:

- (i) All the other eight parameters are fixed as their central values shown in Table II. Then, for a given value of Δ , we vary firstly the value of β_{V_1} in the range of $(0.099 - \Delta, 0.099 + \Delta)$. For each value of β_{V_1} , we calculate the χ^2_{best} .
- (ii) We collect these sets of β_{V_1} , such that the corresponding χ^2_{best} are below $\chi^2_{\text{min}} + 1$. With these collected sets of β_{V_1} , we obtain the standard deviation of parameter β_{V_1} , which is quoted in Table II (in the brackets) as its statistical error.
- (iii) In the same way, we get the errors for all the other parameters.

In Fig. 4 we depict the effective form factor of the Ξ^- and Ξ^0 using the fitted parameters of fit C shown in Table II. The red curve stands for the results of Ξ^0 , while the green curve is the fitted results for Ξ^- . We also show the statistical error bands for the fitted results. Again, one can see that the experimental data on the effective form factors of Ξ^- and Ξ^0 can be well reproduced. It is worth to mention that the two resonances V_1 and V_2 are crucial to describe the experimental data, and without their contributions, we cannot get a good fit to the experimental data. In addition, the total cross section of $e^+e^- \rightarrow \Xi^-\bar{\Xi}^+$ and $e^+e^- \rightarrow \Xi^0\bar{\Xi}^0$ are also calculated with the fitted parameters shown in Table II, and the numerical results are shown Fig. 5. The two peaks of V_1 and V_2 can be clear seen, and more precise data around 2742 MeV and 2993 MeV are needed to further study their properties.

TABLE II. Fitted model parameters for the effective form factors of Ξ^- and Ξ^0 . See more details about the parameters errors of fit C in the text.

Parameter	Fit A	Fit B	Fit C
$\beta_{\omega\phi}$	0.708 ± 0.407	-0.270 ± 0.314	$-0.774 \pm 0.426(0.023)$
$\alpha_{\omega\phi}$	-62.624 ± 13.961	-12.497 ± 11.337	$9.346 \pm 14.501(0.837)$
β_ρ	0.717 ± 0.020	0.328 ± 0.044	$0.616 \pm 0.676(0.024)$
β_{V_1}	$0.099 \pm 0.775(0.003)$
α_{V_1}	$-0.039 \pm 0.76(0.003)$
β_{V_2}	...	-0.047 ± 0.027	$0.115 \pm 0.102(0.002)$
α_{V_2}	...	0.053 ± 0.025	$-0.113 \pm 0.071(0.002)$
M_{V_1} (GeV)	$2.742 \pm 0.015(0.007)$
Γ_{V_1} (MeV)	$71 \pm 59(28)$
χ^2/dof	2.27	1.70	0.29

We next pay attention to the EMFFs at the spacelike region, which can be straightforwardly obtained with these parameters determined from the experimental data in the timelike region. Since the EMFFs in the spacelike region are real, we have to ignore the widths of the vector mesons. Then one can calculate the mean squared charge radius, which is defined by the relation [1,40,55]

$$\langle r_{\text{ch}}^2 \rangle = \begin{cases} \frac{-6}{G_E(0)} \frac{dG_E(Q^2)}{dQ^2} \Big|_{Q^2=0}, & \text{for } \Sigma^+, \Sigma^- \text{ and } \Xi^-, \\ -6 \frac{dG_E(Q^2)}{dQ^2} \Big|_{Q^2=0}, & \text{for } \Sigma^0 \text{ and } \Xi^0, \end{cases} \quad (28)$$

with $Q^2 = -q^2$. With the parameters fitted above, the calculated results of $\langle r_{\text{ch}}^2 \rangle$ of Σ and Ξ hyperons are shown in Table III, where their errors are obtained with the uncertainties of the fitted parameters. Our result for Σ^- is agreement with the experimental data within uncertainties: $\langle r_{\text{ch}}^2 \rangle_{\Sigma^-} = 0.61 \pm 0.12 \pm 0.09$ [1], $\langle r_{\text{ch}}^2 \rangle_{\Sigma^-} = 0.91 \pm 0.32 \pm 0.4$ [2]. In Ref. [1] the Σ^- charge radius was measured in the

spacelike Q^2 range 0.035–0.105 GeV² by elastic scattering of a Σ^- beam off atomic electrons. The measurement was performed with the SELEX (E781) spectrometer using the Fermilab hyperon beam at a mean energy of 610 GeV. In Ref. [2] it was attracted from the elastic scattering of high-energy Σ^- off electrons from carbon and copper targets using the CERN hyperon beam, where these events are identified using a maximum likelihood technique exploring the kinematical relations of the scattered particles. Theoretical calculations with chiral perturbation theory (ChPT) [40,56] and the nonlocal chiral effective theory (ChET) [57], and chiral constituent quark model (ChCQM) [58] are also listed for comparison. One can see that the orderings of the most charge radii calculated by other works are in agreement with our results. Moreover, our results are consistent with these calculations in Refs. [56–58] that $\langle r_{\text{ch}}^2 \rangle_{\Sigma^+} > \langle r_{\text{ch}}^2 \rangle_{\Sigma^-}$. On the contrary, the results obtained with chiral perturbation theory predictions in Ref. [40] indicate that the charge radius of Σ^- is

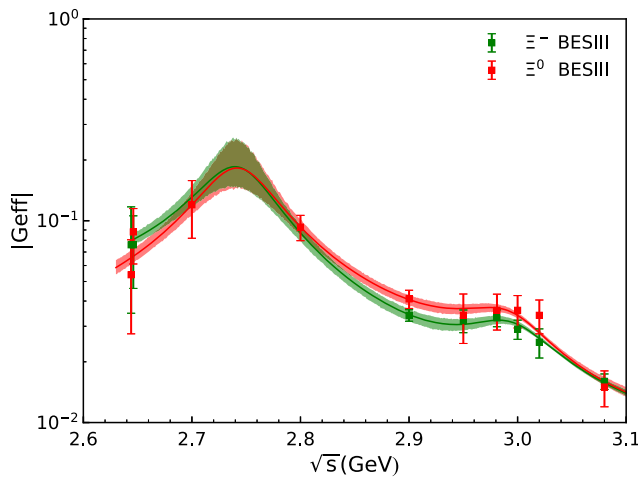


FIG. 4. The obtained Ξ^- and Ξ^0 effective form factors of fit C compared with the experimental data. The bands are obtained from the corresponding statistical errors of the fitted parameters.

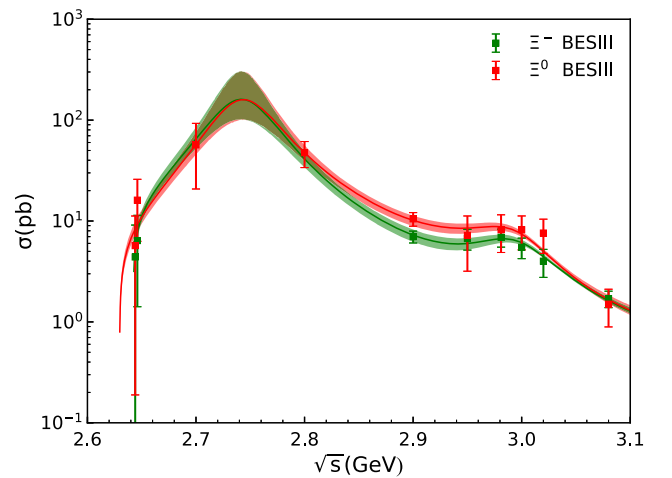


FIG. 5. The obtained total cross sections of $e^+e^- \rightarrow \Xi^-\bar{\Xi}^+$ and $e^+e^- \rightarrow \Xi^0\bar{\Xi}^0$ reactions with the fitted parameters of fit C compared with experimental data. The bands are obtained from the corresponding statistical errors of the fitted parameters.

TABLE III. The obtained results for mean squared electromagnetic radii $\langle r_{\text{ch}}^2 \rangle$ (fm²) for Σ and Ξ. The results from two ChPT calculations, ChET and, ChCQM are also listed.

Baryon	Ξ ⁰	Ξ ⁻	Σ ⁺	Σ ⁰	Σ ⁻
This work	-0.04 ± 0.01	0.58 ± 0.01	0.80 ± 0.02	0.10 ± 0.01	0.70 ± 0.02
ChPT [40]	0.13 ± 0.03	0.49 ± 0.05	0.60 ± 0.02	-0.03 ± 0.01	0.67 ± 0.03
ChPT [56]	0.36 ± 0.02	0.61 ± 0.01	0.99 ± 0.03	0.10 ± 0.02	0.780
ChET [57]	-0.015 ± 0.007	0.601 ± 0.127	0.719 ± 0.116	0.010 ± 0.004	0.700 ± 0.124
ChCQM [58]	0.091	0.587	0.825	0.089	0.643

larger than the one of Σ⁺. In addition, the charge radius of Ξ⁰ calculated here is small and negative, which is in agreement with the nonlocal chiral effective theory calculation in Ref. [57]. It is expected that these results can be tested by future experimental measurements.

IV. SUMMARY

In this work, we study the effective form factor of Σ and Ξ hyperons in timelike region within the vector meson dominance model, and we take a common model parameter γ. In addition, the effect of the isospin combination is taken into account. For the case of Σ hyperon, the contributions from ρ, ω and ϕ mesons are considered. Within same model parameters, we can simultaneously describe the current experimental data on the effective form factors of Σ⁺, Σ⁰, and Σ⁻, while for the case of Ξ⁺ and Ξ⁻, in addition to the contributions of the ground states ρ, ω, and ϕ, it is found that one needs also contributions from two new vector states, and their masses and widths are $M_{V_1} = 2.742$ GeV, $\Gamma_{V_1} = 71$ MeV, $M_{V_2} = 2.993$ GeV, and $\Gamma_{V_2} = 88$ MeV. It is expected that new precise experimental data at BESIII [59] can be used to further study their properties. Especially, more data points around the V_1 peak are crucial

to check the importance of the inclusion of the new state V_1 .

Finally, we would like to stress that thanks to the effects of the isospin combinations, the effective form factors of Σ⁺, Σ⁰, and Σ⁻ can be simultaneously reproduced within the same model parameters by using the vector meson dominance model. Again, the theoretical results obtained here also indicate that the vector meson dominance model is a valid tool for studying the baryonic electromagnetic form factors at the timelike region. More precise data on the $e^+e^- \rightarrow Y\bar{Y}$ reactions can be used to improve our knowledge of hyperon effective form factors and excited vector mesons with mass above 2 GeV.

ACKNOWLEDGMENTS

We warmly thank Professors Xiong-Fei Wang and Xiao-Rong Zhou for useful comments and discussions. We appreciate the anonymous referee for critical comments and suggestions, which were valuable in improving the presentation of the present work. This work is partly supported by the National Natural Science Foundation of China under Grants No. 12075288, No. 11735003, and No. 11961141012. It is also supported by the Youth Innovation Promotion Association CAS.

[1] I. M. Gough Eschrich *et al.* (SELEX Collaboration), *Phys. Lett. B* **522**, 233 (2001).
 [2] M. I. Adamovich *et al.* (WA89 Collaboration), *Eur. Phys. J. C* **8**, 59 (1999).
 [3] M. K. Jones *et al.* (Jefferson Lab Hall A Collaboration), *Phys. Rev. Lett.* **84**, 1398 (2000).
 [4] O. Gayou *et al.* (Jefferson Lab Hall A Collaboration), *Phys. Rev. Lett.* **88**, 092301 (2002).
 [5] M. Ablikim *et al.* (BESIII Collaboration), *Phys. Rev. D* **97**, 032013 (2018).
 [6] M. Ablikim *et al.* (BESIII Collaboration), *Phys. Rev. Lett.* **124**, 032002 (2020).
 [7] M. Ablikim *et al.* (BESIII Collaboration), *Phys. Rev. D* **103**, 012005 (2021).
 [8] M. Ablikim *et al.* (BESIII Collaboration), *Phys. Lett. B* **820**, 136557 (2021).
 [9] M. Ablikim *et al.* (BESIII Collaboration), *Phys. Lett. B* **814**, 136110 (2021).
 [10] M. Ablikim *et al.* (BESIII Collaboration), *Phys. Lett. B* **831**, 137187 (2022).
 [11] X. Wang and G. Huang, *Symmetry* **14**, 65 (2022).
 [12] Belle Collaboration, [arXiv:2210.16761](https://arxiv.org/abs/2210.16761).
 [13] M. A. Belushkin, H. W. Hammer, and U. G. Meissner, *Phys. Rev. C* **75**, 035202 (2007).
 [14] E. A. Kuraev, E. Tomasi-Gustafsson, and A. Dbeyssi, *Phys. Lett. B* **712**, 240 (2012).
 [15] I. T. Lorenz, H. W. Hammer, and U. G. Meißner, *Phys. Rev. D* **92**, 034018 (2015).

- [16] A. Mangoni, S. Pacetti, and E. Tomasi-Gustafsson, *Phys. Rev. D* **104**, 116016 (2021).
- [17] F. Iachello, A. D. Jackson, and A. Lande, *Phys. Lett. B* **43B**, 191 (1973).
- [18] F. Iachello and Q. Wan, *Phys. Rev. C* **69**, 055204 (2004).
- [19] R. Bijker and F. Iachello, *Phys. Rev. C* **69**, 068201 (2004).
- [20] Y. Yang, D. Y. Chen, and Z. Lu, *Phys. Rev. D* **100**, 073007 (2019).
- [21] Z. Y. Li, A. X. Dai, and J. J. Xie, *Chin. Phys. Lett.* **39**, 011201 (2022).
- [22] J. Haidenbauer, U. G. Meißner, and L. Y. Dai, *Phys. Rev. D* **103**, 014028 (2021).
- [23] E. Tomasi-Gustafsson and M. P. Rekalo, *Phys. Lett. B* **504**, 291 (2001).
- [24] A. Bianconi and E. Tomasi-Gustafsson, *Phys. Rev. Lett.* **114**, 232301 (2015).
- [25] A. Bianconi and E. Tomasi-Gustafsson, *Phys. Rev. C* **93**, 035201 (2016).
- [26] M. Ablikim *et al.* (BESIII Collaboration), *Nat. Phys.* **17**, 1200 (2021).
- [27] A. X. Dai, Z. Y. Li, L. Chang, and J. J. Xie, *Chin. Phys. C* **46**, 073104 (2022).
- [28] Q. H. Yang, L. Y. Dai, D. Guo, J. Haidenbauer, X. W. Kang, and U. G. Meißner, *arXiv:2206.01494*.
- [29] X. Cao, J. P. Dai, and H. Lenske, *Phys. Rev. D* **105**, L071503 (2022).
- [30] G. P. Lepage and S. J. Brodsky, *Phys. Rev. Lett.* **43**, 545 (1979); **43**, 1625(E) (1979).
- [31] G. P. Lepage and S. J. Brodsky, *Phys. Rev. D* **22**, 2157 (1980).
- [32] Z. Y. Li and J. J. Xie, *Commun. Theor. Phys.* **73**, 055201 (2021).
- [33] C. F. Perdrisat, V. Punjabi, and M. Vanderhaeghen, *Prog. Part. Nucl. Phys.* **59**, 694 (2007).
- [34] A. Denig and G. Salme, *Prog. Part. Nucl. Phys.* **68**, 113 (2013).
- [35] S. Pacetti, R. Baldini Ferroli, and E. Tomasi-Gustafsson, *Phys. Rep.* **550**, 1 (2015).
- [36] V. Punjabi, C. F. Perdrisat, M. K. Jones, E. J. Brash, and C. E. Carlson, *Eur. Phys. J. A* **51**, 79 (2015).
- [37] A. Mangoni, *SciPost Phys. Proc.* **10**, 021 (2022).
- [38] M. Irshad, D. Liu, X. Zhou, and G. Huang, *Symmetry* **14**, 69 (2022).
- [39] M. Anselmino, E. Predazzi, S. Ekelin, S. Fredriksson, and D. B. Lichtenberg, *Rev. Mod. Phys.* **65**, 1199 (1993).
- [40] B. Kubis and U. G. Meissner, *Eur. Phys. J. C* **18**, 747 (2001).
- [41] M. Ablikim *et al.* (BESIII Collaboration), *Phys. Rev. Lett.* **124**, 042001 (2020).
- [42] L. Xia, C. Rosner, Y. D. Wang, X. Zhou, F. E. Maas, R. B. Ferroli, H. Hu, and G. Huang, *Symmetry* **14**, 231 (2022).
- [43] X. Zhou, L. Yan, R. B. Ferroli, and G. Huang, *Symmetry* **14**, 144 (2022).
- [44] B. Aubert *et al.* (BABAR Collaboration), *Phys. Rev. D* **73**, 012005 (2006).
- [45] B. Aubert *et al.* (BABAR Collaboration), *Phys. Rev. D* **76**, 092006 (2007).
- [46] R. G. Sachs, *Phys. Rev.* **126**, 2256 (1962).
- [47] J. R. Green, J. W. Negele, A. V. Pochinsky, S. N. Syritsyn, M. Engelhardt, and S. Krieg, *Phys. Rev. D* **90**, 074507 (2014).
- [48] S. Dobbs, A. Tomaradze, T. Xiao, K. K. Seth, and G. Bonvicini, *Phys. Lett. B* **739**, 90 (2014).
- [49] J. Haidenbauer, X. W. Kang, and U. G. Meißner, *Nucl. Phys.* **A929**, 102 (2014).
- [50] A. B. Arbuzov and T. V. Kopylova, *J. High Energy Phys.* **04** (2012) 009.
- [51] R. Baldini, S. Pacetti, A. Zallo, and A. Zichichi, *Eur. Phys. J. A* **39**, 315 (2009).
- [52] R. Baldini Ferroli, S. Pacetti, and A. Zallo, *Eur. Phys. J. A* **48**, 33 (2012).
- [53] Q. F. Cao, H. R. Qi, Y. F. Wang, and H. Q. Zheng, *Phys. Rev. D* **100**, 054040 (2019).
- [54] R. L. Workman *et al.* (Particle Data Group), *Prog. Theor. Exp. Phys.* **2022**, 083C01 (2022).
- [55] H. Atac, M. Constantinou, Z. E. Meziani, M. Paolone, and N. Sparveris, *Nat. Commun.* **12**, 1759 (2021).
- [56] A. N. Hiller Blin, *Phys. Rev. D* **96**, 093008 (2017).
- [57] M. Yang and P. Wang, *Phys. Rev. D* **102**, 056024 (2020).
- [58] G. Wagner, A. J. Buchmann, and A. Faessler, *Phys. Rev. C* **58**, 3666 (1998).
- [59] M. Ablikim *et al.* (BESIII Collaboration), *Chin. Phys. C* **44**, 040001 (2020).